# Application of Imaging Flow Cytometry for the Characterization of Intracellular Attributes in Chinese Hamster Ovary Cell Lines at the Single Cell Level

Eva Pekle[1,2], Andrew Smith[1], Guglielmo Rosignoli[1], Christopher Sellick[1,3], C. Mark Smales*[2], Claire Pearce[1,3]

[1]MedImmune, Granta Park, Cambridge, CB21 6GH, UK

[2]Industrial Biotechnology Centre and School of Biosciences, University of Kent, Canterbury, Kent, CT2 7NJ, UK

[3]Current address: Kymab, The Bennet Building B930, Babraham Research Campus, Cambridge, CB22 3AT, UK

*Corresponding author: C. Mark Smales; email c.m.smales@kent.ac.uk

**Keywords**: Chinese hamster ovary (CHO) cells, Single cell imaging, Imaging flow cytometry, organelles

**Abbreviations:**

**CHO**, Chinese hamster ovary; **FACS**, fluorescence activated cell sorting; **IC**, intracellular; **IFC**, imaging flow cytometry; **IS**, ImageStream; **HC**, heavy chain; **LC**, light chain; **mAbs**, monoclonal antibodies

**Abstract**

Biopharmaceutical manufacturing using Chinese hamster ovary (CHO) cells requires the generation of high-producing clonal cell lines. During cell line development, cell cloning using fluorescence activated cell sorting (FACS) has the potential to combine isolation of single cells with sorting based on specific cellular attributes that correlate with productivity and/or growth, identifying cell lines with desirable phenotypes for manufacturing. This study describes the application of imaging flow cytometry (IFC) to characterize recombinant cell lines at the single cell level to identify cell attributes predictive of productivity. IFC assays to quantify organelle content, and recombinant heavy (HC) and light (LC) chain polypeptide and mRNA amounts in single cells were developed. The assays were then validated against orthogonal standard flow cytometry, western blot and qRT-PCR methods. We describe how these IFC assays may be used in cell line development and show how cellular properties can be correlated with productivity at the single cell level, allowing the isolation of such cells during the cloning process. Our analysis found HC polypeptide and mRNA to be predictive of productivity early in the culture, however specific organelle content did not show any correlation with productivity.

## 1. Introduction

Mammalian cells are the expression system of choice for the manufacture of therapeutic glycoproteins, such as monoclonal antibodies (mAbs), with over 70% being produced using CHO cells [1]. During cell line development, random integration of the expression plasmid and host cell heterogeneity results in varied expression levels, requiring extensive screening to identify highly productive clones [2-4]. Strategies to identify cells with increased probability of a high final titre at the cloning step could reduce timelines and diminish the total number of cell lines required to be screened at later stages to isolate such clones. FACS is commonly used for cell cloning in cell line development, having the advantage of being a high-throughput

method that can deposit single cells into wells of multi-well plates, supporting the regulatory demands for clonality, and assess cellular characteristics at the single-cell level. Combining FACS with post-sorting visualisation by fluorescent imaging showed that >99.5% of cells were clonal [5, 6]. Various flow cytometry-based screening methods have been developed to enable selective isolation of high producing clones. These include the capture of secreted mAb via binding to the cell surface using microbead technology , surface affinity matrix , introducing fluorescent markers into the vector and vector modifications to enable secreted mAb to bind to cell surface proteins [10, 11]. Although such approaches give enrichment of high producing clones, they tend be labour intensive and time consuming.

Recent advances in flow cytometry have been made with the development of a novel imaging flow cytometer, ImageStream (IS, Amnis/Merck). A key feature of the IS is that it combines the workflow and high throughput of conventional flow cytometers with the acquisition of up to 12 images per cell, enabling the spatial resolution and determination of quantitative morphology that can be achieved with microscopy [12]. IFC images that may be obtained include side-scatter, brightfield and up to nine fluorescent images, and such data has been used in a range of studies including assessing nuclear translocation [13], detection and discrimination of tumour cells and FISH studies [12]. The current study describes a novel approach to study recombinant CHO cell lines using IFC technology to identify cellular characteristics that correlate with productivity at the single cell level.

## 2. Materials and Methods

### 2.1 Cell culture

CHO cell lines stably expressing a recombinant IgG1 kappa were grown in proprietary medium supplemented with 50 µM methionine sulfoximine (Sigma-Aldrich) and routinely sub cultured as previously described [14].

### 2.2 mAb quantitation

IgG content in clarified culture medium was quantified by protein-A HPLC affinity chromatography on an Agilent HP1100 instrument (Agilent Technologies).

### 2.3 IC HC and LC quantification by western blot

Intracellular polypeptide was assessed using standard western analysis [14]. Membranes were incubated overnight with anti-IgG (FC) antibody conjugated to HRP or anti-kappa conjugated to HRP diluted at 1:10,000 (both from The Binding site). Rabbit anti-GAPDH antibody (Cell Signalling Technology) with a secondary anti-rabbit antibody conjugated to HRP (Jackson ImmunoResearch) was used to detect GAPDH. Blots were developed by incubation with ECL reagent (GE Healthcare Life Sciences) which was also used to measure band intensity for semi-quantitation of proteins.

### 2.4 HC and LC mRNA qPCR

Total RNA was extracted using an RNeasy kit and treated with DNase (Qiagen). qRT-PCR was performed as previously reported [14].

### 2.5 Flow cytometry assays

For HC and LC protein, cells ($1 \times 10^6$) were fixed using a 1:1 solution of Fixation Medium A (Invitrogen) and flow cytometry buffer (PBS with 5% BSA) for 15 min at RT and then incubated with Permeabilisation Medium B (Invitrogen) containing 1:20 goat f(ab')$_2$ anti-human IgG Alexa Fluor conjugated to 488 (Invitrogen, excitation/emission: ~500/520 nm) and goat f(ab')$_2$ anti-human kappa conjugated to APC (Biolegend, excitation/emission: ~650/675 nm) for 15 min, before being washed and analysed. HC and LC mRNA were investigated using a PrimeFlow RNA kit with custom probes (Affymetrix, Merck) following the manufacturer protocol. Quantitation of organelles was performed by staining with Golgi-ID Green (excitation/emission: ~450/530 nm), ER-ID red (excitation/emission: ~580/660 nm),

Mito-ID red (excitation/emission: ~558/690 nm; all from Enzo Life Sciences) and MitoTracker Deep Red (Invitrogen, excitation/emisssion: ~644/665 nm) using the manufacturers' protocols. DAPI (excitation/emisssion: ~340/450 nm) or Sytox nuclear (excitation/emission: ~444/480) counter-stain were used for nuclear localization.

**2.6 Flow cytometry**

Flow cytometry was performed on a BD Canto flow cytometer with the BD FACSDiva™ software. Cells were stained with DAPI and MitoTracker and excited with a violet (405 nm) and red (633 nm) laser and 10,000 events acquired for each sample. Doublets and debris were removed by gating on forward and side scatter dot plots. FlowJo software was used for statistical analysis.

**2.7 IFC**

An ImageStream® imaging flow cytometer (Merck) with INSPIRE® software was used to collect 10,000 events (or 10 min acquisition time). Images of each event were captured using a 60X objective with 405, 488 and 658 nm lasers, collecting fluorescent images in channels 7, 2 and 5 respectively, alongside channel 1 and 9 for brightfield and channel 6 for darkfield. Cell classifier was set to 50 on area-lower limit on the brightfield channel to avoid debris acquisition. Analysis was performed using IDEAS® software (v6.2). Compensation settings were calculated using the built-in software algorithm in best-fit mode, and refined manually. Focused cells were gated using the plot of contrast versus gradient RMS features and single cells were gated using a dot plot of the aspect ratio versus cell area for the brightfield channel.

**3. Results and Discussion**

The first step in this study was to develop IFC assays to investigate the content of intracellular (IC) HC and LC polypeptide, HC and LC mRNA, and specific cellular organelles (Fig. 1A).

Key features of the IFC software are functions that enable spot counting (Fig. 1B) to quantify punctate staining, such as the Golgi, and masking to determine cell or organelle size by creating a mask on the brightfield image (Fig. 1C). Additionally, co-localization between two signals can also be determined (Fig. 1D).

Standard flow cytometry is widely accepted as a robust method for investigating cellular attributes, however IFC is a relatively new technology and has not been as extensively used. We therefore assessed the reproducibility and consistency of results between standard flow cytometry and IFC. To do this, three separate vials of a recombinant CHO cell line were thawed and independently cultured in shake flasks. After the first passage, triplicate samples were taken from each flask on three separate days and stained with MitoTracker and DAPI (Fig. 2A). The percentage of double positive cells across instruments and days, ranged from 94.8% to 100% (Fig. 2B-C). Intensity of nuclear and mitochondrial staining was consistent across instruments (Fig. 2D-G), with a good correlation between the signal intensity recorded by the different instruments for both dyes (Fig. 2 H, I; $R^2$= 0.42 DAPI and 0.97 MitoTracker), giving confidence that observations by IFC could be transferred to standard flow cytometry.

To investigate cellular differences between high/low producing cell lines, and correlations between organelle content and cell culture parameters, a panel of 19 cell lines expressing a model IgG1 mAb with a range of titres, specific productivities and growth in fed-batch culture was used (Supplementary Table 1). IC HC and LC polypeptide and mRNA expression varied across the cell lines but also within individual cell lines at different timepoints of fed-batch culture (Fig. 3 and Supplementary Table 2). The amounts of HC polypeptide and mRNA on day 4, as determined by western blotting and qPCR respectively, were both predictive of final titre (Fig. 3A-B), as well as overall qP (data not shown), HC polypeptide and qP, Pearson's correlation coefficient R = 0.77, and for HC mRNA, R = 0.82). No correlation was found between titre and LC content (data not shown) or between HC

polypeptide and titre later in the culture (days 7 and 9). From these results, IC HC polypeptide and mRNA on day 4 could be used as markers of cellular productivity.

IC HC and LC polypeptide and mRNA content was then assessed using IFC. HC polypeptide and mRNA content on day 3 showed a strong correlation with final titre (Fig. 3C, D), but at later time points (days 6 and 10), no such correlation was found. This suggests that IC HC polypeptide and mRNA content are predictive of final titre early in fed-batch culture, however, this predictive power is lost as the culture progresses as other factors begin to play a role in determining final titre, e.g. availability of translation machinery, folding/secretion and energy status of cell. LC polypeptide amounts showed no correlation with final titer or qP, although LC mRNA showed a positive correlation with final titer ($R = 0.73$ on day 3). Overall, these results are consistent with previous reports that IC HC polypeptide and mRNA content show a stronger correlation with mAb productivity than LC content, indicating that HC can be a limiting factor of final titre [15-20]. Although the correlation with LC was lower, there was some correlation between LC transcript and final titre, this not being unexpected as LC polypeptide is necessary to drive HC constant domain 1 (CH1) folding, mAb assembly and secretion [21, 22]. The reported differences as to whether HC or LC are limiting may reflect molecule-dependent and host cell-dependent differences. We note that the cell line with the highest HC mRNA content on day 3 did not have the highest titre. This cell line also had a high amount of LC mRNA on day 6, suggesting that above a certain transcript threshold, there might be potential bottlenecks further down the translation and secretion pathways [14, 16, 23].

Next, we investigated multiplexing HC mRNA and HC polypeptide assays at the single cell level and this revealed a positive correlation with titre, similar to that seen at the population level with qRT-PCR and western blotting assays (Fig 3E). IFC images revealed differential cytoplasmic localisation of the HC polypeptide and HC mRNA, consistent with previous findings of HC polypeptide residing in the ER and Golgi [24], and mRNA localised with

ribosomes on the ER surface (Fig. 3F). As both HC mRNA and polypeptide show a positive correlation with final titre early in culture and with each other, HC polypeptide was selected as the marker of productivity at the single cell level as the assay is more time and cost efficient than that for mRNA. HC polypeptide was then multiplexed with assays for different organelles.

Differences in productivity between cell lines can be explained by a diverse range of mRNA levels, but also by differences in cellular properties that govern the growth and biosynthetic capacities of individual clones. Energy metabolism [25] and the protein synthesis [16], folding and secretion pathways can influence the final production and secretion of mAb. We therefore investigated with IS whether productivity differences observed between cell lines was correlated with variations in the mitochondria, ER and Golgi content of cells, as well as HC and LC polypeptide and mRNA. Correlations were investigated at the population (population median intensity vs. final titre for all cell lines) and single cell (intensity organelle vs. intensity HC) level (Supplementary Table 2). No linear correlations were found for individual cell lines between the mitochondrial content and HC polypeptide or mRNA amounts at the single cell level on any sampled days. Moreover, no relationships were found at the population level between mitochondrial content and productivity, or specific productivity on any of the days investigated. Mitochondrial content itself is not always reflective of cellular metabolism, as significant changes in the mitochondrial membrane potential (MMP) can occur without fluctuations in mitochondria numbers [28-30]. Studies have linked either high [29] or low [28] MMP with increased final titre, however we only considered mitochondrial biomass in this study.

Additionally, no correlations were observed between HC content and ER content at the single cell level or at the population level between the ER or Golgi content and titre or specific productivity (Supplementary Table 2). Other studies report similar findings during the growth phase [1, 15] whilst our results show neither the ER content nor the Golgi content correlate

with productivity during the growth phase or at later stages of batch culture. We note reports that host cells with higher ER content prior to transfection result in the isolation of recombinant cells with higher titre [31].

IFC currently has limitations in its application to sorting and isolation of cells in a cell line construction process. Currently IFC does not offer a high spatial resolution compared to traditional microscopes, which also allow for time-lapse experiments, and spatial-temporal analysis of the sample [32]. A further limitation of IFC is its maximum speed of 300 events/sec, which can only be reached with a high sample concentration of $10^8$ cells/mL. This is quite different to the high-throughput of standard flow cytometry. The slow acquisition is mostly the result of limitations in focusing of cells, as out of focus cells are excluded from analysis [32]. Finally, there are currently no commercially available IFCs that have the ability to sort cells based on image-features, although that may change in the near future following the recent work by Nitta et al. on intelligent image-activated cell sorting [33].

Whilst the limitations are evident, the powerful IFC approach described here has the potential to identify novel cellular attributes that could be implemented to select for high producing cells (and eventually cells that have optimal growth profiles and specific product quality profiles) during the cell line development process. Single cell analysis by IFC could be combined with other approaches such as O-propargyl-puromycin labelling to investigate correlations between organelle content, HC and LC transcript and polypeptide and total protein synthesis rate [34]. As new live cell assays become available, further characterization of other cell characteristics can be investigated and correlated with desirable cell culture attributes such as productivity, growth or product quality.

In this study of a panel of 19 cell lines, no differences in organelle content were observed between high and low producers of a model mAb that is considered easy-to-express. However, it is possible that cellular organelle amounts might differentiate between productivity

capability of cell lines making more difficult-to-express molecules. Moreover, the IFC tools described here could be applied to characterization of host cell populations and to identify potential targets for host cell engineering. Consistent with previous reports, we show that HC protein and mRNA are markers of productivity early in culture: this highlights a need for the development of new flow cytometric methods that allow the measurement of HC polypeptide or mRNA amounts in live cells, which could be used to enrich the proportion of high producers and improve the efficiency of cell line development.

**Acknowledgements**

The authors would like to acknowledge Dr Sarah Dunn for stable cell line generation, Dr Charlotte Godfrey for initial characterisation of the cell lines and Dr Diane Hatton for manuscript review.

**Conflict of Interest Statement**

The authors declare no commercial or financial conflict of interest.

## References


[1] D. Reinhart, L. Damjanovic, C. Kaisermayer, R. Kunert, *Appl. Microbiol. Biotechnol.* **2015**, *99*, 4645-4657.
[2] S. Misaghi, D. Shaw, S. Louie, A. Nava, L. Simmons, B. Snedecor, C. Poon, J. S. Paw, L. Gilmour-Appling, J. E. Cupp, *Biotechnol. Prog.* **2016**, *32*, 198-207.
[3] W. Pilbrough, T. Munro, P. Gray, *PloS ONE* **2009**, *4*.
[4] J. F. Povey, C. J. O'Malley, T. Root, E. B. Martin, G. A. Montague, M. Feary, C. Trim, D. A. Lang, R. Alldread, A. J. Racher, C. M. Smales, *J. Biotechnol.* **2014**, *184*, 84-93.
[5] J. Fieder, P. Schulz, I. Gorr, H. Bradl, T. Wenger, *Biotechnol J* **2017**, *12(6)* doi: 10.1002/biot.201700002.
[6] K. Evans, T. Albanetti, R. Venkat, R. Schoner, J. Savery, G. Miro-Quesada, B. Rajan, C. Groves, *Biotechnol. Progr.* **2015**, *31*, 1172-1178.
[7] K. T. Powell, J. C. Weaver, *Biotechnol.* **1990**, *8*, 333-337.
[8] R. Manz, M. Assenmacher, E. Pfluger, S. Miltenyi, A. Radbruch, *Proc. Natl Acad. Sci. U.S.A* **1995**, *92*, 1921-1925.
[9] R. J. Sleiman, P. P. Gray, M. N. McCall, J. Codamo, N. A. Sunstrom, *Biotechnol. Bioeng.* **2008**, *99*, 578-587.
[10] B. Yu, J. M. Wages, J. W. Larrick, *Protein Eng. Des. Sel.* **2014**, *27*, 309-315.
[11] S. Lang, D. Drewello, J. Wichter, A. Nommay, B. Wilms, H. P. Knopf, T. Jostock, *Biotechnol. Bioeng.* **2016**, *113*, 2386-2393.
[12] D. A. Basiji, W. E. Ortyn, L. Liang, V. Venkatachalam, P. Morrissey, *Clin. Lab. Med.* **2007**, *27*, 653-670.
[13] T. C. George, S. L. Fanning, P. Fitzgerald-Bocarsly, R. B. Medeiros, S. Highfill, Y. Shimizu, B. E. Hall, K. Frost, D. Basiji, W. E. Ortyn, P. J. Morrissey, D. H. Lynch, *J. Immunol. Methods* **2006**, *311*, 117-129.
[14] C. L. Godfrey, E. J. Mead, O. Daramola, S. Dunn, D. Hatton, R. Field, G. Pettman, C. M. Smales, *Biotechnol. J.* **2017**, *12(8)*, doi: 10.1002/biot.201700177.
[15] R. Z. Edros, S. McDonnell, M. Al-Rubeai, *PloS ONE* **2013**, *8*, e75935.
[16] E. J. Mead, R. J. Masterton, M. Feary, O. Obrezanova, L. Zhang, R. Young, C. M. Smales, *Biochem. J.* **2015**, *472*, 261-273.
[17] N. Borth, K. Strutzenberger, U. Donalies, R. Kunert, H. Katinger, *Cytotechnology* **1996**, *22*, 129-138.
[18] J. McLeod, P. M. O'Callaghan, L. P. Pybus, S. J. Wilkinson, T. Root, A. J. Racher, D. C. James, *Biotechnol. Bioeng.* **2011**, *108*, 2193-2204.
[19] P. M. O'Callaghan, J. McLeod, L. P. Pybus, C. S. Lovelady, S. J. Wilkinson, A. J. Racher, A. Porter, D. C. James, *Biotechnol. Bioeng.* **2010**, *106*, 938-951.
[20] N. Borth, D. Mattanovich, R. Kunert, H. Katinger, *Biotechnol. Prog.* **2005**, *21*, 106-111.
[21] H. Dorai, B. Csirke, B. Scallon, S. Ganguly, *Hybridoma* **2006**, *25*, 1-9.
[22] K. Strutzenberger, N. Borth, R. Kunert, W. Steinfellner, H. Katinger, *J. Biotechnol.* **1999**, *69*, 215-226.
[23] V. Chromikova, A. Mader, W. Steinfellner, R. Kunert, *Cytotechnology* **2015**, *67*, 343-356.
[24] S. Mathias, S. Fischer, R. Handrick, J. Fieder, P. Schulz, H. Bradl, I. Gorr, M. Gamer, K. Otte, *J. Biotechnol.* **2018**, *271*, 47-55.
[25] CA. Sellick, A. S. Croxford, A. R. Maqsood, G. Stephens, H. V. Westerhoff, R. Goodacre, A. J. Dickson, *Biotechnol. Bioeng.* **2011**, *108*, 3025-3031.
[26] C. Mohan, G. M. Lee, *Biotechnol. Bioeng.* **2010**, *107*, 337-346.
[27] A. Tastanova, A. Schulz, M. Folcher, A. Tolstrup, A. Puklowski, H. Kaufmann, M. Fussenegger, *J. Biotechnol.* **2016**, *219*, 72-85.
[28] G. Hinterkorner, G. Brugger, D. Muller, F. Hesse, R. Kunert, H. Katinger, N. Borth, *J. Biotechnol.* **2007**, *129*, 651-657.

[29] L. Chakrabarti, A. Mathew, L. Li, S. Han, J. Klover, T. Albanetti, P. Hawley-Nelson, *J. Immunol. Methods* **2018**. pii: S0022-1759(18)30192-3.
[30] N. Borth, G. Kral, H. Katinger, *Cytometry* **1993**, *14*, 70-73.
[31] P.M. O'Callaghan, M.E. Berthelot, R.J. Young, J.W. Graham, A.J. Racher, D. Aldana, *Biotechnol. Progr.* **2015**, *31*, 1187-1200.
[32] N. S. Barteneva, E. Fasler-Kan, I. A. Vorobjev, *J. Histochem. Cytochem.* **2012**, *60*, 723-733.
[33] N. Nitta, T. Sugimura, A. Isozaki, H. Mikami, K. Hiraki, S. Sakuma, T. Iino, F. Arai, T. Endo, Y. Fujiwaki, H. Fukuzawa, M. Hase, T. Hayakawa, K. Hiramatsu, Y. Hoshino, M. Inaba, T. Ito, H. Karakawa, Y. Kasai, K. Koizumi, S. Lee, C. Lei, M. Li, T. Maeno, S. Matsusaka, D. Murakami, A. Nakagawa, Y. Oguchi, M. Oikawa, T. Ota, K. Shiba, H. Shintaku, Y. Shirasaki, K. Suga, Y. Suzuki, N. Suzuki, Y. Tanaka, H. Tezuka, C. Toyokawa, Y. Yalikun, M. Yamada, M. Yamagishi, T. Yamano, A. Yasumoto, Y. Yatomi, M. Yazawa, D. Di Carlo, Y. Hosokawa, S. Uemura, Y. Ozeki, K. Goda, *Cell* **2018**, *175*, 266-276 e213.
[34] F. Nagelreiter, M. T. Coats, G. Klanert, E. Gludovacz, N. Borth, J. Grillari, M. Schosserer, *Biotechnol. J.* **2018**, *13*, e1700492.

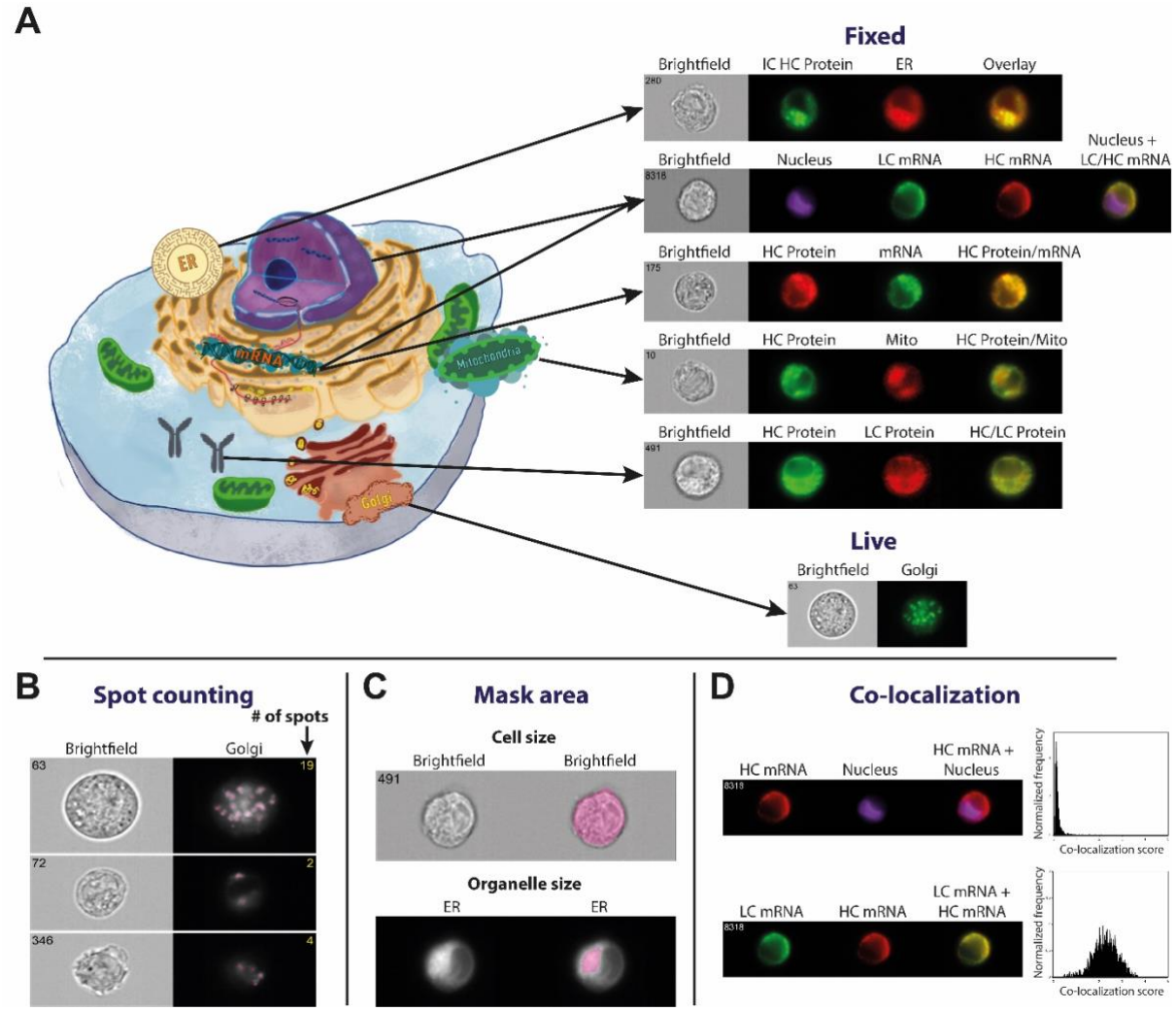


Fig. 1. Sample images of the assays developed on the ImageStream. (A) Assays were developed in fixed cells for multiplexing with HC protein detection. The assays include ER, LC and HC mRNA, LC and HC polypeptide, and mitochondria. The Golgi assay was developed in live cells. Images show brightfield, fluorescent staining and an overlay of the staining. (B) Sample images featuring spot counting of the Golgi apparatus, with brightfield and fluorescent channel images with the number of spots on the right corner of the image. (C) Masking of the cell size based on the brightfield image, and of organelle size based on the threshold of the ER intensity. (D) Co-localization of HC mRNA and nucleus, which shows no co-localization, and HC and LC mRNA which show strong co-localization.

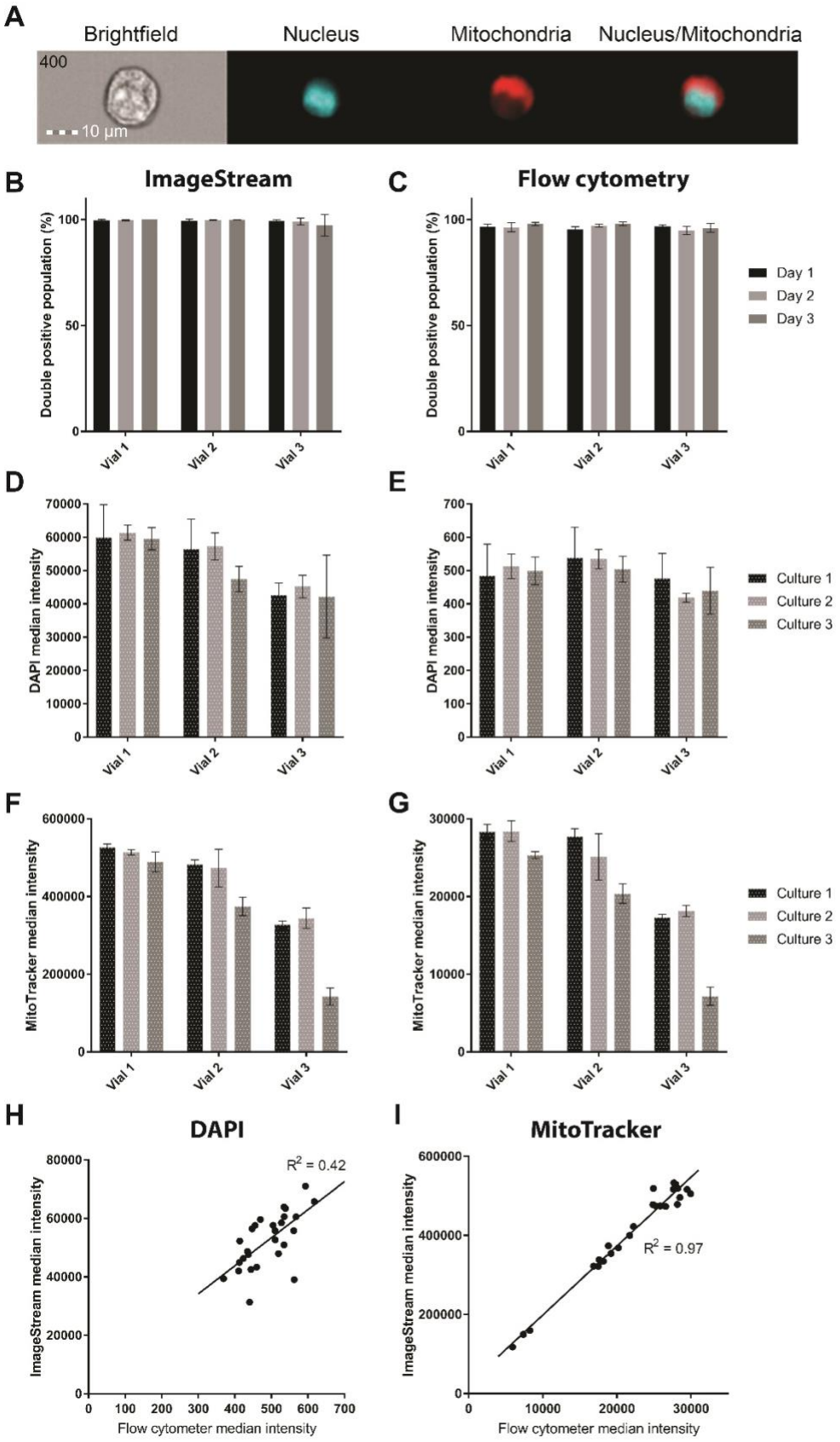
A
Brightfield
Nucleus
Mitochondria
Nucleus/Mitochondria
400
10 µm
B
ImageStream
Double positive population (%)
Vial 1
Vial 2
Vial 3
C
Flow cytometry
Day 1
Day 2
Day 3
D
DAPI median intensity
E
Culture 1
Culture 2
Culture 3
F
MitoTracker median intensity
G
H
DAPI
$R^2$ = 0.42
ImageStream median intensity
Flow cytometer median intensity
I
MitoTracker
$R^2$ = 0.97

Fig. 2. (A) Sample ImageStream images showing the brightfield, nuclear staining (DAPI), mitochondria staining (MitoTracker) and composite image. (B & C) Average percentage of cells positive for both nuclear and mitochondrial staining for each vial on different days on ImageStream (B) and flow cytometry (C). (D-G) Average of DAPI median intensity (D, E) and MitoTracker median intensity (F, G) of individual shake flasks on day 3, representative of observations on other days, for ImageStream (D, F) and flow cytometry (E, G). The intensity of the nuclear staining was consistent between instruments and between shake flasks originating from the same vial, showing no statistical difference (Fig. 2D-E). For the mitochondrial staining, differences in intensity were present between shake flasks originating from the same vial and between vials, which could be due to intrinsic differences between cultures (Fig. 2F-G). Cultures were prepared and analysed in a different order to avoid order bias. Overall, there was a strong correlation between the signal measured by both instruments (Pearson's correlation coefficient $R = 0.65$ for nuclear stain and $R = 0.98$ for mitochondrial stain). (H & I) DAPI median intensity of individual samples from day 3 (H) and MitoTracker (I) from flow cytometer versus ImageStream, with the R-squared values (coefficient of determination) on the graph and Pearson correlation coefficients of 0.65 and 0.98, respectively.

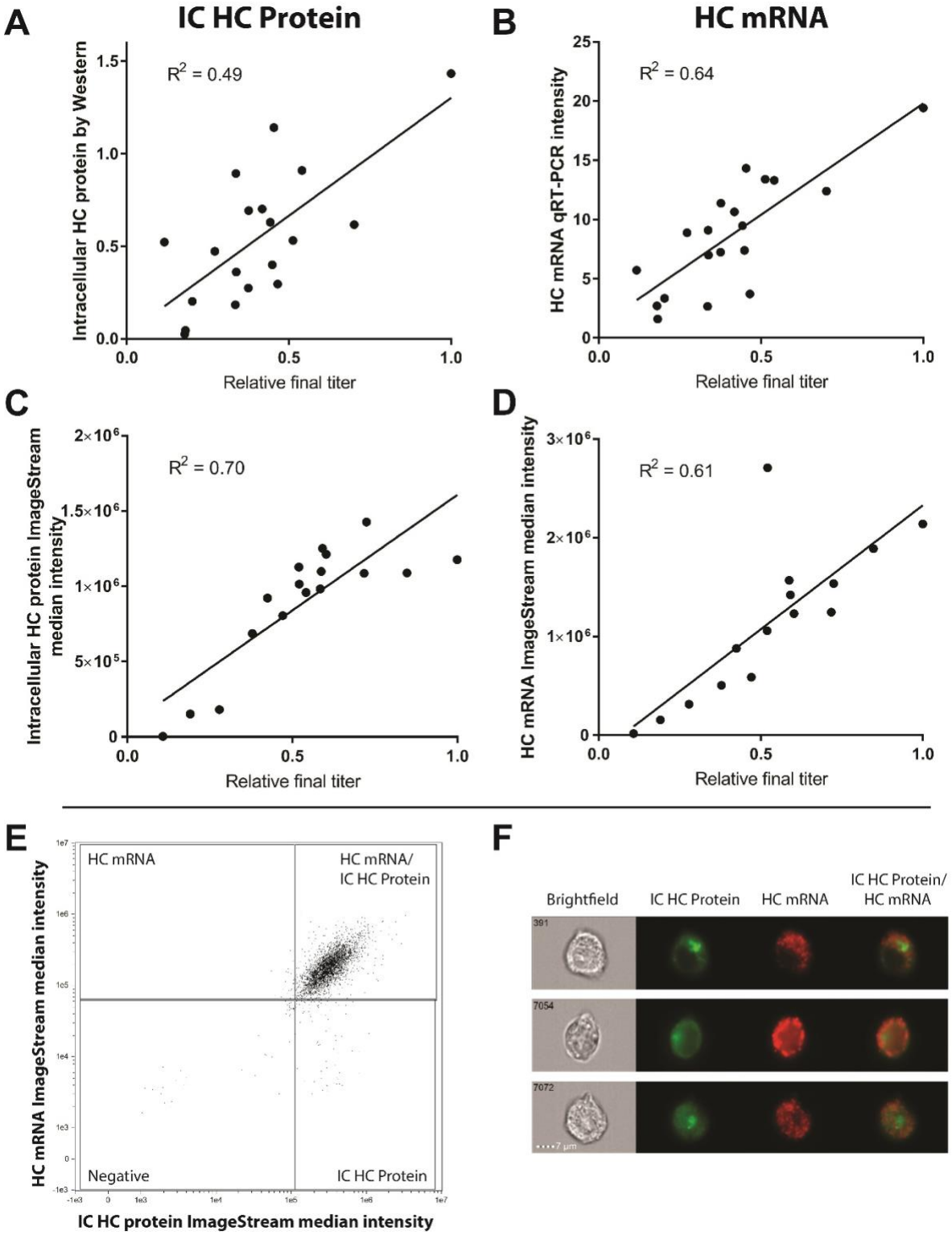


Fig. 3. (A, C) Correlation between titre and IC HC protein measured by western blotting (A) and IFC (C) ($R^2$ = 0.84 where $R^2$ is the coefficient of determination.). (B, D) Correlation between titre and HC mRNA measured by qRT-PCR (B) and IFC (D) (R = 0.79). (E, F) Multiplexing of HC mRNA and polypeptide with IFC (R = 0.65 for E)

Supplementary Table 1: Productivity and growth values for the 19 characterized cell lines in fed-batch culture.

| Cell line | qP (pg / cell / day) | Titer (mg / L) | IVC (*$10^6$ cells / ml) |
|---|---|---|---|
| **19** | 10.2 | 859 | 67 |
| **5** | 9.9 | 1326 | 153 |
| **3** | 6.4 | 1343 | 224 |
| **1** | 4.9 | 1496 | 303 |
| **4** | 28.8 | 2014 | 83 |
| **2** | 10.7 | 2485 | 237 |
| **18** | 28.8 | 2494 | 94 |
| **10** | 14.9 | 2505 | 152 |
| **8** | 8.6 | 2778 | 324 |
| **16** | 20.7 | 2789 | 155 |
| **11** | 22.0 | 3098 | 163 |
| **17** | 31.0 | 3281 | 127 |
| **14** | 11.3 | 3327 | 325 |
| **13** | 18.8 | 3364 | 188 |
| **15** | 12.3 | 3450 | 319 |
| **9** | 34.1 | 3800 | 127 |
| **6** | 24.2 | 4007 | 167 |
| **12** | 27.8 | 5201 | 206 |
| **7** | 74.5 | 7418 | 118 |

Supplementary Table 2: Pearson's correlation coefficient between the organelle content on different days and the cell culture growth and productivity values. The last column provides the range of the Pearson's correlation coefficient on individual clones between HC and mitochondrial or ER content at the single cell level.

| | **Final titre** | **qP** | **Final IVC** | **Viability** | **HC protein (single cell level)** |
|---|---|---|---|---|---|
| **Mitochondrial content** | | | | | |
| **d3** | -0.22 | -0.04 | -0.32 | -0.44 | 0.03 to 0.52 |
| **d6** | 0.23 | 0.25 | -0.69 | -0.37 | 0.02 to 0.46 |
| **d10** | -0.03 | 0.09 | -0.07 | 0.18 | - 0.03 to 0.49 |
| **ER content** | | | | | |
| **d3** | 0.16 | 0.36 | -0.64 | -0.38 | -0.12 to 0.54 |
| **d6** | 0.12 | 0.40 | -0.43 | -0.38 | -0.9 to 0.51 |
| **d10** | -0.48 | -0.4 | 0.36 | 0.72 | -0.16 to 0.58 |
| **Golgi content** | | | | | |
| **d6** | -0.11 | 0.26 | -0.48 | -0.41 | |
| **d10** | -0.49 | -0.27 | 0.18 | 0.61 | |
| **HC mRNA** | | | | | |
| **d3** | 0.79 | 0.92 | -0.44 | -0.38 | |
| **d6** | 0.31 | 0.55 | -0.51 | -0.32 | |
| **LC mRNA** | | | | | |
| **d3** | 0.58 | 0.83 | -0.62 | -0.42 | |
| **d6** | 0.12 | 0.34 | -0.35 | -0.26 | |
| **HC protein** | | | | | |
| **d3** | 0.84 | 0.60 | -0.41 | 0.11 | |
| **d6** | 0.02 | -0.11 | 0.46 | 0.47 | |
| **d10** | 0.12 | 0.06 | -0.13 | 0.19 | |
| **LC protein** | | | | | |
| **d3** | 0.61 | 0.44 | -0.90 | 0.22 | |
| **d6** | -0.02 | -0.03 | 0.32 | 0.47 | |
| **d10** | 0.06 | -0.03 | -0.27 | -0.10 | |